Activation analysis of rapid thermally annealed Si and Mg implanted semi-insulating GaAs

J. L. Tandon and I. S. Leybovich
McDonnell Douglas Astronautics Company, Huntington Beach, California 92647

G. Bai
California Institute of Technology, Pasadena, California 91125

(Received 8 February 1989; accepted 15 May 1989)

Electronic properties of Si and Mg implants in undoped semi-insulating GaAs are studied. The activation of the implants is achieved by rapid thermal annealing. The effects of implantation dose and anneal temperature on the measured electrical activity are investigated. In spite of similar depth distributions and implantation damage characteristics, a marked difference between the activations of the Si and the Mg ions is observed for the dose range considered (3×10^{12}–1×10^{14} cm^{-2}). Lattice strain measurements performed by x-ray rocking curves indicate that the residual implantation damage after annealing is not largely responsible for this difference. The difference is mostly electronic in character, as also suggested by photoluminescence measurements. At high annealing temperatures, changes in the compensating properties of undoped semi-insulating GaAs are suspected, and are found to play an important role in the activation of implanted ions, affecting the *n*- and *p*-type dopants conversely.

I. INTRODUCTION

Complementary integrated circuits in GaAs require both *n*- and *p*-type regions on the same wafer. With isolation provided by the high-resistivity of semi-insulating GaAs, such regions can be most conveniently generated by selective implantations and appropriate masking.[1,2] The use of the ion implantation technique thus considerably simplifies the fabrication of these circuits.

In order to control the characteristics of *n*- and *p*-type devices constituting the complementary circuits, the electrical properties of the implanted layers should be properly tailored and well understood. The implantation of ions, by itself, is generally well controlled. It is the post-implantation annealing conditions which often impose problems and demand attention. Annealing following implantation is invariably necessary for removal of implantation damage and electrical activation of the ions. When both *n*- and *p*-type ions are implanted into the same wafer, annealing conditions become even more critical because they have to be compatible for both *n*- and *p*-type dopants.

In this paper, the characteristics of implanted Si(*n*-type) and Mg(*p*-type) ions in undoped semi-insulating GaAs are discussed. Si and Mg are specially chosen because of their closeness in atomic masses. The damage created in GaAs by the two ions is thus nearly identical. The post-implantation annealing is carried out by rapid thermal annealing (RTA). As well documented,[3–5] RTA offers many advantages when compared to conventional furnace annealing. Due to short times involved, the integrity of implanted depth profiles can be better preserved. Also, requirements on caps to protect the GaAs surface from dissociation are less stringent.

A combined study of rapid thermally annealed Si and Mg implants in semi-insulating GaAs is particularly useful for optimizing implant and anneal conditions for fabricating both *n*- and *p*-type devices on the same wafer. In addition, this study also provides insight into the role the properties of undoped semi-insulating GaAs may play in affecting the electrical activity of the implants, which is crucial for the control and reproducibility of device characteristics.

II. EXPERIMENTAL METHODS

$^{28}Si^{+}$ and $^{24}Mg^{+}$ ions were implanted at room temperature in commercially available liquid encapsulated Czochralski (LEC) grown undoped ⟨100⟩ semi-insulating GaAs. The energies of the implants were selected to be 70 keV for Si^{+} and 55 keV for Mg^{+} ions, to yield approximately the same projected range for the two ions. The dose range investigated for both ions was from 3×10^{12} to 1×10^{14} cm^{-2}. This range is typically used in fabricating *n* and *p* field effect transistors (FET's). After implantation the wafers were coated with an ~1000-Å-thick silicon nitride film deposited by reactive sputtering. Small (~1×1 cm) samples cleaved from the coated wafers were then annealed at different temperatures in an AG Heatpulse 410 system with a forming gas ambient. During annealing the samples were placed on a Si wafer, and the temperature of the cycle was monitored and controlled by a thermocouple welded to a Si test-chip located close by inside the annealing chamber. The temperature values reported in the paper are those measured by the thermocouple on the Si test chip. Considering differences in the optical absorption properties between Si and GaAs, the reported temperature values are expected to differ somewhat from the actual values of the annealed samples. The true temperature of the GaAs sample during annealing is difficult to establish, and is estimated to be 20–50 °C lower than the cycle temperature. As measured by the Si test-chip thermocouple, all annealings were carried out with a temperature rise rate of ~100 °C/s, and in the cycle the samples were held at the reported final temperature for 5 s, before cool down. In all cases, even after 1000 °C annealings, the silicon

 0734-211X/89/051090-06$01.00

nitride films adhered well to GaAs, with no observable signs of cracking or blistering.

Following annealing, the silicon nitride films were removed by etching in a CF_4–O_2 plasma. The electrical activity in the samples was determined by Hall effect measurements with alloyed indium contacts. Lattice strain in the samples was monitored by Bragg-case double-crystal x-ray rocking curves with the Fe $K\alpha_1$ (400) symmetric reflection. The x-ray beam was collimated and rendered nearly monochromatic by (400) reflection in ⟨100⟩ GaAs. The lattice strain is indicative of damage introduced by ion implantation. Standard photoluminescence (PL) measurements were carried out at ~5 K using an Ar^+ ion laser ($\lambda = 514.5$ nm) as an excitation source. The PL spectra provide information about the radiative energy-level transitions in the implanted and annealed samples.

III. RESULTS

A. Electrical activation measurements

The electrical activations of the implanted ions are represented by the ratio of the sheet free-carrier concentrations (N_S or P_S) to the ion dose (N_I). A ratio of one thus corresponds to a 100% activation.

In Fig. 1, the ratio N_S/N_I is plotted against N_I for Si implants. The three curves are for three different annealing temperatures. For the dose range considered (3×10^{12}–1×10^{14} cm^{-2}), each of the N_S/N_I curves pass through a maximum. Implants with doses $(1.5–3)\times10^{13}$ cm^{-2} result in highest activation, and the level somewhat increases with increasing temperature. One of the striking features of Fig. 1 is the fact that on either side of the maxima of the N_S/N_I curves, the dependence on annealing temperature is opposite. High temperatures result in improved activation of high-dose implants, whereas low temperatures are favorable for low-dose implants. From the point of view of implant damage removal, high temperatures are expected to enhance activation.[6] However, a decrease in activation with an increase of temperature, as observed for low dose implants, is rather surprising. In fact, a sample implanted with 3×10^{12} cm^{-2} and annealed at 900 °C is almost semi-insulating in electrical activity.

A more elaborate account of the activation behavior of Si implants is given in Fig. 2. In this figure, the ratio N_S/N_I is plotted against annealing temperature. The three curves are for three different doses. Once again, for doses of 5×10^{12} and 2.2×10^{13} cm^{-2}, peaks in the activation are observed. Maximum activation occurs at higher temperatures for higher doses. Also, beyond peak activiation, lower doses suffer loss of electrical activity at lower temperatures, with the resistivity of the samples ultimately approaching that of semi-insulating GaAs. The curve for the 1×10^{14} cm^{-2} implants barely reaches to its maximum value at 1000 °C, and its behavior appears to be similar to those of the 5×10^{12} and the 2.2×10^{13} cm^{-2} implants. The fact that the maximum N_S/N_I for the 1×10^{14} cm^{-2} implants is lower, when compared to the 5×10^{12} and the 2.2×10^{13} cm^{-2} implants, is most likely due to the saturation of Si activation in GaAs,[7,8] which limits the value of N_S.

In contrast to Si, the electrical activation behavior of Mg implants is quite different. This is shown in Figs. 3 and 4. The ratio of free-hole concentration to implantation dose (P_S/N_I) follows a systematic trend with N_I, decreasing slightly with increasing N_I (Fig. 3). In a similar dose range considered, higher activation is achieved for Mg than Si implants. As depicted in Fig. 4, the effect of anneal temperature on P_S/N_I is not so strong. An important and surprising result emerging from Fig. 4 is that annealing of low-dose (5×10^{12} cm^{-2}) Mg implants at high temperatures (>950 °C) result in P_S/N_I values >1.

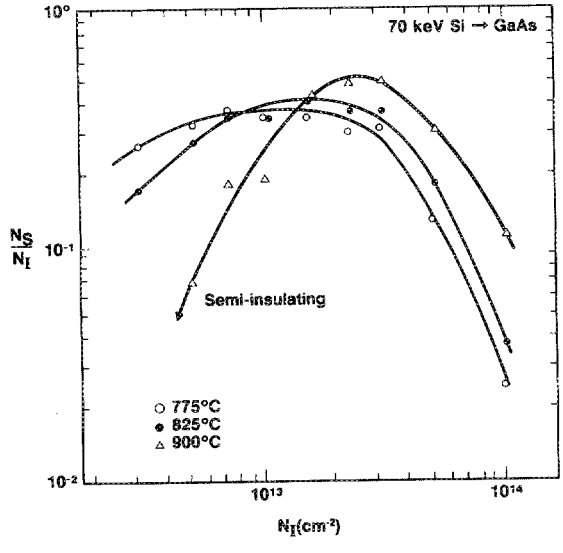

FIG. 1. The ratio of the sheet electron concentration to the ion dose (N_S/N_I) vs the ion dose (N_I) for 70-keV Si implants in GaAs. The three curves are for three different temperatures of annealing.

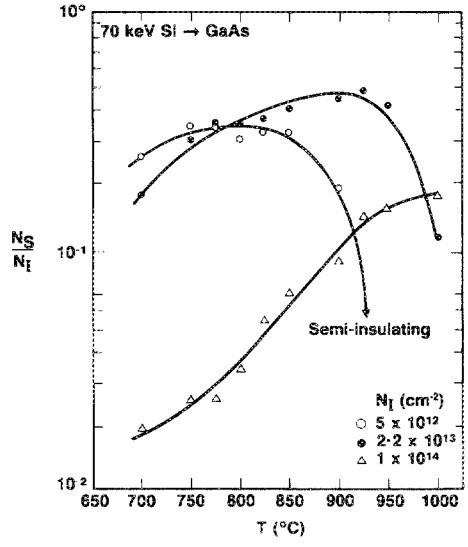

FIG. 2. Activation ratio (N_S/N_I) for Si implants as a function of annealing temperature (T). The three curves are for three different ion doses.

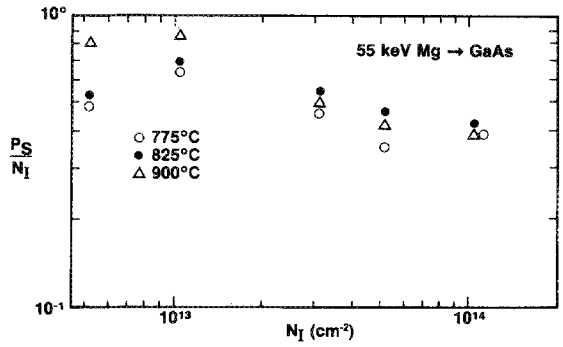

FIG. 3. The ratio of the sheet hole concentration to the ion dose (P_S/N_I) vs the ion dose (N_I) for 55-keV Mg implants in GaAs. Data obtained on samples annealed at three different temperatures is plotted.

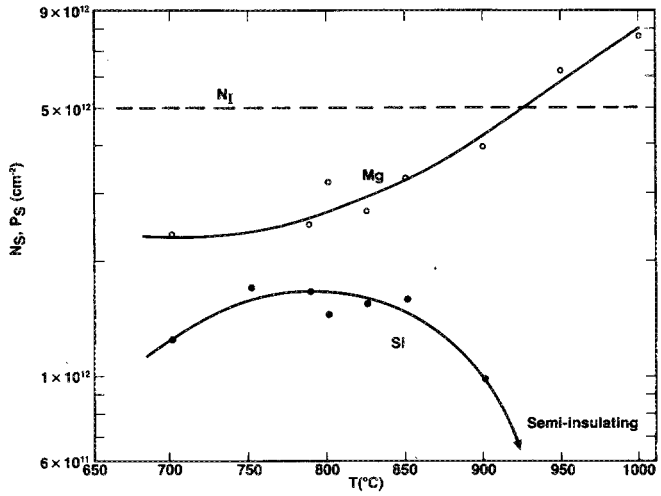

FIG. 5. N_S and P_S as a function of annealing temperature for Si and Mg implants, respectively. Both Si and Mg were implanted to a dose of 5×10^{12} cm^{-2}. This level is also indicated as N_I by dotted lines.

The unusual activations of low-dose (5×10^{12} cm^{-2}) Si and Mg implants, as a function of annealing temperature, are replotted together in Fig. 5, for further clarity. Here N_S and P_S are plotted for Si and Mg implants, respectively, against annealing temperature. It is interesting to note that the Si and Mg data are consistent with each other: at high annealing temperatures when Si-implanted samples approach semi-insulating characteristics, Mg-implanted samples exhibit P_S values greater than the implanted dose. This behavior is discussed later in the paper after analyzing x-ray rocking curve measurements and photoluminescence data.

B. X-ray rocking curve measurements

Lattice strain measurements made by x-ray rocking curves are extremely sensitive in detecting damage created by ion implantation. Some of the rocking curves obtained on Si implanted and annealed samples are depicted in Fig. 6, for the conditions as shown. The power of the reflected Fe $K\alpha_1$ x-ray beam is plotted against the relative rocking angle ($\Delta\theta$), which is normalized with respect to the Bragg-case reflection for single-crystal GaAs at $\Delta\theta = 0°$. For (400) reflections, a symmetric peak at $\Delta\theta = 0°$ thus represents signal from a good quality single-crystal ⟨100⟩ GaAs. Strain resulting from ion implantation damage is quite apparent from the rocking curves obtained on the as-implanted samples. The additional asymmetric features at $\Delta\theta < 0°$ are due to this strain. As expected, increased damage with increased implantation dose results in more pronounced strain. Details on the relationship between damage and strain are described elsewhere.[9,10]

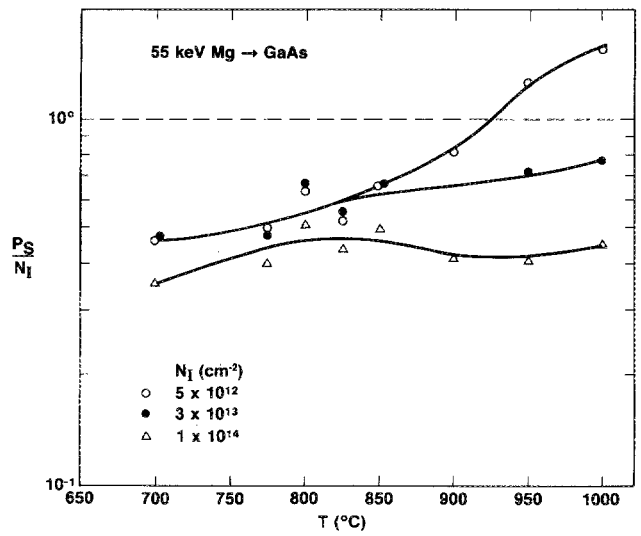

FIG. 4. Activation ratio (P_S/N_I) for Mg implants as a function of annealing temperature (T). The three curves are for three different ion doses.

Rocking curves obtained on Si implanted samples after annealing are also shown in Fig. 6. As observed, an anneal temperature of 800 °C is sufficient to remove all implantation damage from both of the 5×10^{12} and the 2.2×10^{13} cm^{-2} implanted samples. Further annealing at 1000 °C results in no detectable change in the rocking curves, indicating that no additional annealing-induced crystalline damage is introduced upon 1000 °C annealing. In both cases, after 800 or 1000 °C annealing, the crystalline quality of the samples is as good as unimplanted single-crystal GaAs.

Similar implantation damage and annealing characteristics were also observed for the Mg-implanted samples.

C. Photoluminescence (PL) measurements

PL Spectra were obtained to determine optically excited energy-level transitions in unimplanted and implanted samples, before and after annealing.

Figure 7 shows typical spectra collected on unimplanted undoped semi-insulating GaAs. The as-received material has several identifiable peaks. The cluster of peaks ~1.515 eV is due to excitonic transitions in GaAs.[11] As suggested in literature,[12,13] the peaks at 1.491 and 1.494 eV may be related to carbon impurity, with 1.491 eV representing a neutral-

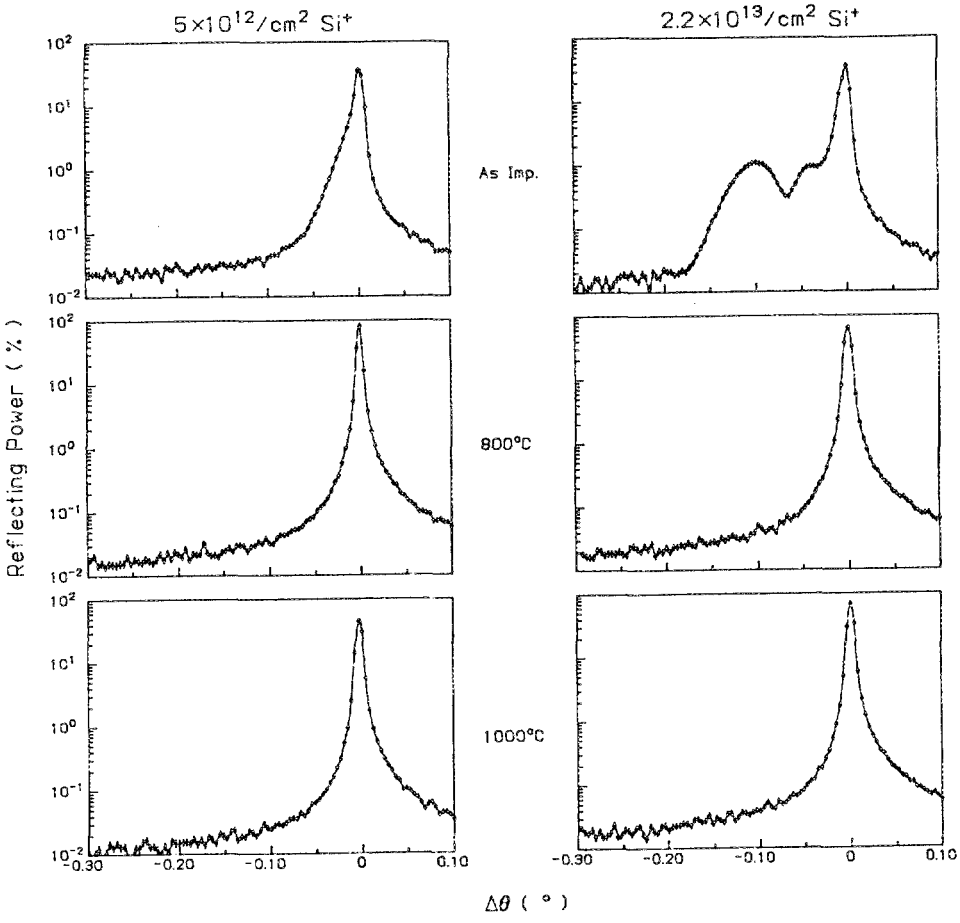

FIG. 6. (400) Fe $K\alpha_1$ x-ray rocking curves collected on some of the Si-implanted and annealed samples. (See text for details.)

donor–neutral-carbon acceptor (D°–C°) transition and 1.494 eV a free-electron–neutral-carbon acceptor (e–C°) transition. The low-intensity peaks at 1.455 and 1.457 eV are longitudinal optical (LO) phonon replicas of the peaks at 1.491 and 1.494 eV, respectively.

The PL spectrum of the as-received material, as shown in Fig. 7, is found to be characteristic of the LEC grown undoped semi-insulating GaAs. Wafers tested from different manufacturers showed similar general features, except that the relative intensities of the peaks at 1.491 and 1.494 eV varied from wafer to wafer. However, for a particular wafer from a manufacturer, upon annealing with a silicon nitride cap up to at least 950 °C, no significant change in the PL spectrum was observed. Such a typical result for the material used for the studies in this paper is shown in Fig. 7. Anneal-

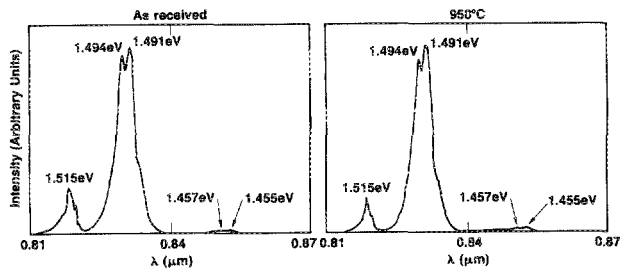

FIG. 7. Typical PL spectra obtained on LEC grown undoped semi-insulating GaAs before and after annealing. The annealing was carried out with an ~1000-Å-thick silicon nitride encapsulant film.

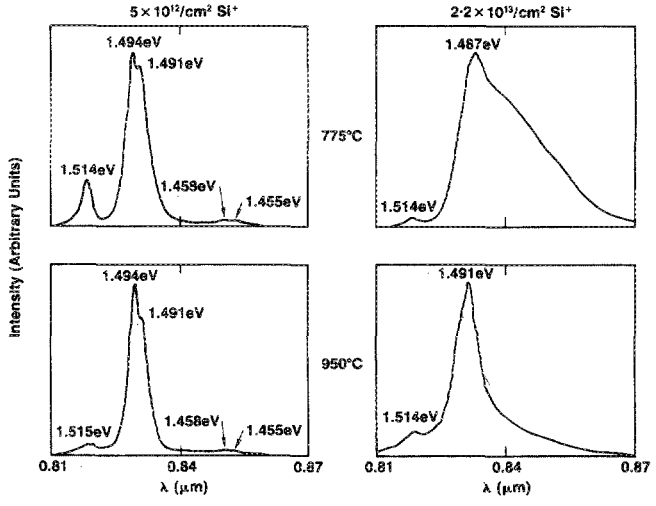

FIG. 8. PL spectra obtained on some of the Si-implanted and annealed samples.

ing of undoped semi-insulating GaAs with a silicon nitride cap thus does not result in any detectable new transition levels, or any changes in the relative intensities of the 1.491 and the 1.494 eV transitions.

Some of the PL spectra obtained on Si implanted and annealed samples are shown in Fig. 8. For the low-dose (5×10^{12} Si^+/cm^2) implanted samples, the spectra are found to possess similar features as the unimplanted case (see Fig. 7). However, with implanted Si impurity and with annealing temperature, the relative intensities of (D°–C°) and (e–C°) transitions change. An increase in annealing temperature also results in the relative supression of excitonic transitions. The reasons for such changes in the PL spectra are not clear yet. Nevertheless, the changes do indicate that the implanted silicon impurity has an influence on the radiative (D°–C°) and (e–C°) transitions present in the original semi-insulating material.

The PL spectra measured on high-dose (2.2×10^{13} Si^+/cm^2) implanted and annealed samples are also shown in Fig. 8. After an annealing temperature of 775 °C, the spectrum is broad, with the peak located at 1.487 eV. The peak at 1.487 eV may be attributed to a free-electron neutral Si acceptor transition (e–Si°). The broad spectrum is indicative of a band of transitions occurring to acceptor level in the band gap of GaAs. Increasing annealing temperature to 950 °C results in a narrow spectrum, with the dominance of the (D°–C°) and the (e–C°) transitions restored. From the PL data it appears that the transition to the Si acceptor level is more readily detectable in the 2.2×10^{13} cm^{-2} implanted samples than the 5×10^{12} cm^{-2} implanted samples. This may be because of higher concentration of Si in the former case. In either case, however, at high annealing temperatures the original (D°–C°) and (e–C°) transitions dominate.

Corresponding PL measurements performed on Mg-implanted and annealed samples are shown in Fig. 9. The transitions to the Mg acceptor level are found to overlap with the (D°–C°) and (e–C°) transitions. The peak at 1.491 eV is strong in all cases. Implantation dose, or the annealing temperature, do not affect the PL spectra signficantly. The weak shoulder in the PL spectrum at 1.494 eV, which becomes apparent for the 5×10^{12} Mg^+/cm^2 implanted sample upon annealing at 1000 °C, may again hint the role of the substrate material in influencing the transitions.

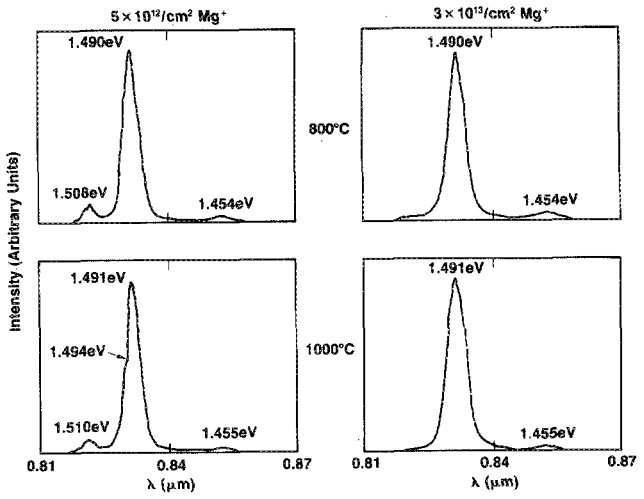

FIG. 9. PL spectra obtained on some of the Mg-implanted and annealed samples.

IV. DISCUSSION

The data presented in this paper demonstrates clear differences between the electrical activation properties of rapid thermally annealed Si and Mg implants in undoped semi-insulating GaAs. Possible reasons for these differences are discussed in this section.

The crystalline damage introduced in GaAs by implanting Si or Mg ions is nearly identical, because of their closeness in masses. As shown by sensitive x-ray rocking curve measurements (Fig. 6) this damage is all annealed out at 800 °C. Also, RTA by itself does not introduce any detectable damage up to at least 1000 °C. Residual implantation damage, present in the samples after annealing, thus does not appear to be the major cause of the observed activation differences between the Si and the Mg implants. The effects of subtle crystalline defects like clusters or dislocation loops, often observed during annealing of high-dose implants,[14] on the activation behavior are expected to be minimum for the dose range considered.

The most striking difference between the activations of Si and Mg ions is revealed during annealing of low-dose implants. This is shown in Fig. 5. At high annealing temperatures, Mg implanted samples exhibit sheet hole concentrations in excess of the implantation dose, whereas Si implanted samples approach semi-insulating characteristics in electrical activity. This consistent behavior can best be interpreted as electronic in origin. The data indicate that additional acceptor levels are generated, or become apparent, in the implanted samples upon annealing. Such acceptor levels, presumably, supply additional free holes in the Mg implanted samples, and correspondingly become effective in compensating the Si implanted samples.

The origin of additional acceptor levels needed to explain the data of Fig. 5 is not clear from the studies performed. Rapid thermal annealing of silicon-nitride-capped unimplanted semi-insulating GaAs up to 1000 °C did not show any p-type conversion. Radiative transitions in the unimplanted material also did not change upon annealing, as measured by PL (see Fig. 7). The results suggest that the additional acceptor levels are perhaps only revealed in the presence of implanted dopants. It appears that the electronic compensation of undoped semi-insulating GaAs is somewhat disturbed upon implantation of electronically active impurities and annealing at high temperatures. Weak evidence to this effect is provided by the PL data on the Si and the Mg implanted and annealed samples (see Figs. 8 and 9). In any event, the net result is revelation of additional acceptor levels that influence the activation of implanted dopants.

In understanding the electrical activation behavior of implanted dopants, the original electronic properties of compensated undoped semi-insulating GaAs, and changes upon annealing, should be considered. This is the main message

provided by the studies performed in this paper. There also seems to be an electronic interaction between implanted dopants and compensating impurities in the semi-insulating material, especially for low concentration levels of implanted impurities. Compensating properties of undoped semi-insulating GaAs, and changes upon annealing, are continually being studied. Evidence exists for the thermal conversion of the material upon annealing, and is attributed to the out-diffusion of Ga,[15] or EL2 compensating levels.[16] However, a relationship between such studies and the activation of implanted dopants still needs to be established.

V. CONCLUSIONS

Electrical activations of rapid thermally annealed Si and Mg implants in undoped semi-insulating GaAs have been studied. A clear difference is observed in the activation behavior of the two ions. The difference is interpreted as electronic in origin, rather than related to residual implantation damage.

A combined study of Si (n-type) and Mg (p-type) implants proves particularly useful in providing insight into the role the compensating properties of undoped semi-insulating GaAs may play in affecting the activation of the implanted ions. Results suggest that, upon annealing, the implanted dopants interact with the compensating characteristics of the undoped semi-insulating GaAs. As a consequence, additional acceptor levels become apparent, which affect the activations of Si and Mg implants conversely.

ACKNOWLEDGMENTS

This work was supported by McDonnell Douglas Corporation's Internal Research and Development funds. Assistance provided by M. C. Stonage and P. E. Friebertshauser with implantations is acknowledged. We also thank J. K. Abrokwah at McDonnell Douglas and M-A. Nicolet at Caltech for their continued interest and encouragement.

[1]R. A. Kiehl, M. A. Sontras, D. J. Widiger, and W. M. Kwapien, IEEE Trans. Electron Devices **34**, 2412 (1987).
[2]R. Zuleeg, J. K. Notthoff, and G. L. Troeger, IEEE Electron Dev. Lett. **5**, 21 (1984).
[3]K. D. Cummings, S. J. Pearton, and G. P. Vella-Coleiro, J. Appl. Phys. **60**, 163 (1986).
[4]S. S. Gill and B. J. Sealy, J. Electrochem. Soc. Solid State Sci. Technol. **133**, 2590 (1986).
[5]See, for example, Rapid Thermal Processing of Electronic Materials, Materials Research Society Symposia Proceedings, Vol. 92; and papers therein, 1987.
[6]J. L. Tandon, M-A. Nicolet, and F. H. Eisen, Appl. Phys. Lett. **34**, 165 (1979).
[7]S. K. Tiku and W. M. Duncan, J. Electrochem. Soc. Solid State Sci. Technol. **132**, 2237 (1985).
[8]T. C. Banwell, M. Maenpaa, M-A. Nicolet, and J. L. Tandon, J. Phys. Chem. Solids **44**, 507 (1983).
[9]B. M. Paine, N. N. Hurvitz, and V. S. Speriosu, J. Appl. Phys. **61**, 1335 (1987).
[10]B. M. Paine and V. S. Speriosu, J. Appl. Phys. **62**, 1704 (1987).
[11]U. Heim and P. Hiesinger, Phys. Status Solidi (B) **66**, 461 (1974).
[12]K. Akimoto, M. Dohsen, M. Arai, and N. Watanabe, Appl. Phys. Lett. **45**, 922 (1984).
[13]D. J. Ashen, P. J. Dean, D. T. J. Hurle, J. B. Mullin, A. M. White, and P. D. Greene, J. Phys. Chem. Solids **36**, 1041 (1975).
[14]M. A. Shahid, R. Bensalem, and B. J. Sealy, Mater. Res. Soc. Symp. Proc. **35**, 489 (1985).
[15]Y. J. Chan and M. S. Lin, J. Appl. Phys. **60**, 2184 (1986).
[16]M. Matsui and T. Kazuno, Appl. Phys. Lett. **51**, 659 (1987).